

Journal of Reinforced Plastics and Composites

<http://jrp.sagepub.com>

A Comparison of 9 and 16 Node Quadrilateral Elements Based on Higher-Order Laminate Theories for Estimation of Transverse Stresses

B.S. Manjunatha and T. Kant

Journal of Reinforced Plastics and Composites 1992; 11; 968

DOI: 10.1177/073168449201100902

The online version of this article can be found at:
<http://jrp.sagepub.com/cgi/content/abstract/11/9/968>

Published by:

 SAGE Publications

<http://www.sagepublications.com>

Additional services and information for *Journal of Reinforced Plastics and Composites* can be found at:

Email Alerts: <http://jrp.sagepub.com/cgi/alerts>

Subscriptions: <http://jrp.sagepub.com/subscriptions>

Reprints: <http://www.sagepub.com/journalsReprints.nav>

Permissions: <http://www.sagepub.com/journalsPermissions.nav>

A Comparison of 9 and 16 Node Quadrilateral Elements Based on Higher-Order Laminate Theories for Estimation of Transverse Stresses

B. S. MANJUNATHA AND T. KANT*
*Department of Civil Engineering
Indian Institute of Technology
Powai, Bombay 400 076
India*

ABSTRACT: C° finite elements based on a set of higher-order theories are projected to provide reliable predictions for interlaminar stresses in layered composite and sandwich laminates. These theoretical-cum-computational models incorporate laminate deformations which account for the effects of transverse shear deformation, transverse normal strain/stress and a nonlinear variation of inplane displacements with respect to the thickness coordinate, thus eliminating the need for shear correction coefficients. The inplane stresses are evaluated via constitutive relations, while the interlaminar stresses are evaluated by using the equilibrium equations. 16 and 9 noded Lagrangian selectively integrated isoparametric elements are used in this study. The present results, when compared with available elasticity and closed-form laminate solutions, show good agreement. New results for sandwich laminates are also presented which may serve as a benchmark for future investigations.

1. INTRODUCTION

IN RECENT YEARS composite materials have been widely used, largely because of their high specific stiffness and strength, excellent damage tolerance and superior fatigue response characteristics. Laminated composites are in increasing demand, because they can be tailored to suit almost any particular application. These laminates are fabricated by stacking up plies or laminae of unidirectional fibrous composites with each lamina oriented in different directions to achieve the required stiffness and strength.

Refined analytical tools are needed for the prediction of the laminate behaviour. Classical lamination theory [1] based on Kirchhoff hypothesis and first-order shear deformation theories due to Reissner [2] and Mindlin [3] have been used to predict laminate response. The classical theory assumes linear variation

*Author to whom all communications should be addressed.

of inplane displacements through the thickness, neglects shear deformation implied by Kirchhoff hypothesis and assumes state of plane stress in the constitutive relations which eliminates the possibility of rigorous calculation of interlaminar stresses. The first-order shear deformable theory based on assumed stress [2] and displacement [3] fields remove some of the defects of the classical theory. However, this theory too neglects the effect of transverse normal strain/stress and is based on a constant transverse shear strain/stress through the laminate thickness. Thus a shear correction coefficient(s) which is somewhat arbitrary is introduced to correct the transverse shear strain energy of deformation. These discrepancies have been rectified in recent years by introducing higher-order functions in the displacement models, thus leading to the development of higher-order laminate theories.

Reissner [4] has given an exact approach to this problem which reproduced the earlier equations of two-dimensional laminate theory and provided new supplementary information concerning certain three-dimensional aspects of the problem. Lo et al. [5] presented closed form solutions for isotropic and laminated plates with a higher-order displacement model. These theories incorporate the effect of transverse normal stress/strain and lead to the realistic variation of transverse shear stress/strain, but fail to eliminate the latter on the bounding planes of the plate. Kant [6] and Kant et al. [7] are the first to present a C^0 finite element formulation of a higher-order theory. This theory considers three-dimensional Hooke's law, incorporates the quadratic variation of the transverse shear strain and linear variation of transverse normal strain through the plate thickness and thus eliminates the need for shear correction coefficient(s).

Murthy [8] and Reddy [9] have adopted a displacement model that neglects the strain energy due to transverse normal stress. Later, Reddy and his co-workers presented closed form solution, C^1 displacement finite element [10] and mixed finite element [11] models of the earlier formulation [9]. But this formulation is computationally inefficient because of C^1 continuity and is not amenable to the popular and widely used isoparametric formulation in present day finite element technology.

In spite of the efforts of these research workers, simple and accurate evaluation of interlaminar shear and normal stresses, an important aspect in the prediction of failure modes under a given set of loading, has not been clearly reported. Kant and his co-workers have given a set of higher-order theories [12–19] which may be used to evaluate interlaminar shear stresses by using 9 noded Lagrangian element. For estimating interlaminar normal stress one has to use the third equilibrium equation which requires the use of third derivative of displacements. Hence, in this present work 16 noded cubic element is developed and used to evaluate interlaminar stresses. These are then compared with the available closed form solutions [20–24].

2. THEORY AND FORMULATION

A number of refined higher-order shear deformable theories for the analysis of anisotropic composite and sandwich laminates are summarized below separately

for symmetric and unsymmetric laminates in the increasing order of their degrees-of-freedom (dof).

2.1 Symmetric Laminates

1. Higher-order shear deformation theory (HOST5A), 5 dof/node

$$\begin{aligned} u(x, y, z) &= z\theta_x(x, y) + z^3\theta_x^*(x, y) \\ v(x, y, z) &= z\theta_y(x, y) + z^3\theta_y^*(x, y) \\ w(x, y, z) &= w_o(x, y) \end{aligned} \quad (1)$$

2. Higher-order shear deformation theory (HOST6A), 6 dof/node

$$\begin{aligned} u(x, y, z) &= z\theta_x(x, y) + z^3\theta_x^*(x, y) \\ v(x, y, z) &= z\theta_y(x, y) + z^3\theta_y^*(x, y) \\ w(x, y, z) &= w_o(x, y) + z^2w_o^*(x, y) \end{aligned} \quad (2)$$

2.2 Unsymmetric Laminates

1. Higher-order shear deformation theory (HOST7A), 7 dof/node

$$\begin{aligned} u(x, y, z) &= u_o(x, y) + z\theta_x(x, y) + z^3\theta_x^*(x, y) \\ v(x, y, z) &= v_o(x, y) + z\theta_y(x, y) + z^3\theta_y^*(x, y) \\ w(x, y, z) &= w_o(x, y) \end{aligned} \quad (3)$$

2. Higher-order shear deformation theory (HOST9), 9 dof/node

$$\begin{aligned} u(x, y, z) &= u_o(x, y) + z\theta_x(x, y) + z^2u_o^*(x, y) + z^3\theta_x^*(x, y) \\ v(x, y, z) &= v_o(x, y) + z\theta_y(x, y) + z^2v_o^*(x, y) + z^3\theta_y^*(x, y) \\ w(x, y, z) &= w_o(x, y) \end{aligned} \quad (4)$$

3. Higher-order shear deformation theory (HOST11), 11 dof/node

$$\begin{aligned} u(x, y, z) &= u_o(x, y) + z\theta_x(x, y) + z^2u_o^*(x, y) + z^3\theta_x^*(x, y) \\ v(x, y, z) &= v_o(x, y) + z\theta_y(x, y) + z^2v_o^*(x, y) + z^3\theta_y^*(x, y) \\ w(x, y, z) &= w_o(x, y) + z\theta_z(x, y) + z^2w_o^*(x, y) \end{aligned} \quad (5)$$

4. Higher-order shear deformation theory (HOST12), 12 dof/node

$$\begin{aligned}
 u(x, y, z) &= u_o(x, y) + z\theta_x(x, y) + z^2u_o^*(x, y) + z^3\theta_x^*(x, y) \\
 v(x, y, z) &= v_o(x, y) + z\theta_y(x, y) + z^2v_o^*(x, y) + z^3\theta_y^*(x, y) \quad (6) \\
 w(x, y, z) &= w_o(x, y) + z\theta_z(x, y) + z^2w_o^*(x, y) + z^3\theta_z^*(x, y)
 \end{aligned}$$

where u , v and w are the displacements of a general point (x, y, z) in the laminate in x , y and z directions, respectively. The parameters u_o , v_o , w_o , θ_x , θ_y and θ_z are the appropriate two-dimensional terms in the Taylor series and are defined in x - y plane at $z = 0$ (Figure 1). The parameters u_o^* , v_o^* , w_o^* , θ_x^* , θ_y^* and θ_z^* are higher-order terms in the Taylor's series expansion and their physical interpretation is difficult indeed, except that they represent higher-order transverse cross-sectional deformation modes.

The strain displacement relations for a point at a distance z from the middle surface of the laminate are given by,

$$\begin{aligned}
 \epsilon_x &= \frac{\partial u}{\partial x} & \epsilon_y &= \frac{\partial v}{\partial y} & \epsilon_z &= \frac{\partial w}{\partial z} \\
 \gamma_{xy} &= \frac{\partial u}{\partial y} + \frac{\partial v}{\partial x} & \gamma_{xz} &= \frac{\partial u}{\partial z} + \frac{\partial w}{\partial x} \quad (7) \\
 \gamma_{yz} &= \frac{\partial v}{\partial z} + \frac{\partial w}{\partial y}
 \end{aligned}$$

Each lamina in the laminate is assumed to be in a three-dimensional stress state so that the constitutive relation for a typical lamina L with reference to the fiber-matrix coordinate axes (1-2-3) can be written as,

$$\begin{bmatrix} \sigma_1 \\ \sigma_2 \\ \sigma_3 \\ \tau_{12} \end{bmatrix} = \begin{bmatrix} C_{11} & C_{12} & C_{13} & 0 \\ & C_{22} & C_{23} & 0 \\ & \text{sym} & & C_{33} \\ & & & C_{44} \end{bmatrix} \begin{bmatrix} \epsilon_1 \\ \epsilon_2 \\ \epsilon_3 \\ \tau_{12} \end{bmatrix} \quad (8)$$

$$\begin{bmatrix} \tau_{23} \\ \tau_{13} \end{bmatrix} = \begin{bmatrix} C_{55} & 0 \\ 0 & C_{66} \end{bmatrix} \begin{bmatrix} \gamma_{23} \\ \gamma_{13} \end{bmatrix} \quad (9)$$

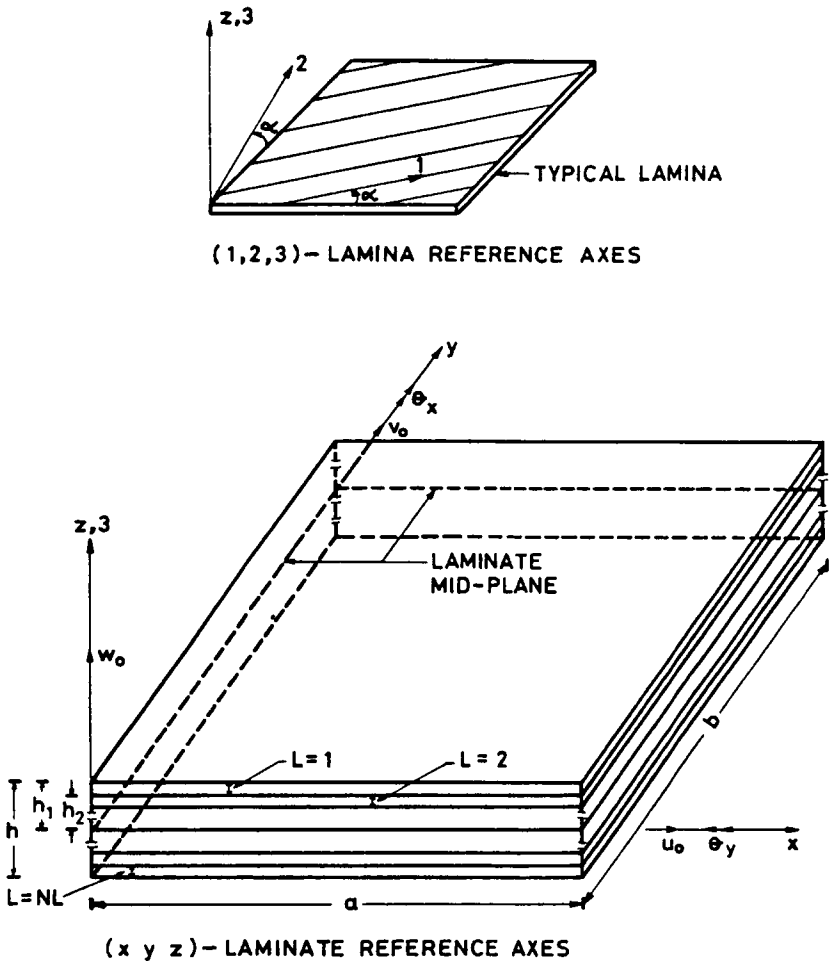


Figure 1. Laminate geometry with positive set of lamina/laminate reference axes, displacement components and fibre orientation.

where $(\sigma_1, \sigma_2, \sigma_3, \tau_{12}, \tau_{23}, \tau_{13})$ are the stress and $(\epsilon_1, \epsilon_2, \epsilon_3, \gamma_{12}, \gamma_{23}, \gamma_{13})$ are the linear strain components referred to the lamina coordinates (1-2-3) and C_{ij} 's are the elastic constants of the L^{th} lamina.

In the laminate coordinates (x, y, z) the stress-strain relations for the L^{th} lamina can be written as

$$\underline{\sigma} = \underline{Q}\underline{\epsilon} \tag{10a}$$

where

$$\underline{\sigma} = [\sigma_x, \sigma_y, \sigma_z, \tau_{xy}, \tau_{yz}, \tau_{xz}]^t \tag{10b}$$

$$\underline{\epsilon} = [\epsilon_x, \epsilon_y, \epsilon_z, \gamma_{xy}, \gamma_{yz}, \gamma_{xz}]^t$$

are stress and strain vectors with respect to the laminate axes and

$$\underline{Q} = \underline{T}^{-1}\underline{C}\underline{T}^{-t} \tag{11}$$

is the three-dimensional elastic constants matrix in the laminate axes of the L^{th} lamina and \underline{T} is the coordinate transformation matrix (see Figure 1). The expressions of elastic constants are defined in Reference [13].

The total potential energy Π of the laminate after an explicit integration is carried out through the thickness is obtained in the following two-dimensional form,

$$\Pi = \frac{1}{2} \int_A \bar{\underline{\epsilon}}^t \bar{\underline{d}} dA - \int_A (\underline{d})^t \underline{p}_o dA \tag{12}$$

in which,

$$\bar{\underline{d}} = (N_x, N_y, N_{xy}, N_x^*, N_y^*, N_{xy}^*, N_z, N_z^*, M_x, M_y, M_{xy}, M_x^*, M_y^*, M_{xy}^*, M_z, Q_x, Q_y, Q_x^*, Q_y^*, S_x, S_y, S_x^*, S_y^*)^t$$

$$\bar{\underline{\epsilon}} = (\epsilon_{x0}, \epsilon_{y0}, \epsilon_{xy0}, \epsilon_{x0}^*, \epsilon_{y0}^*, \epsilon_{xy0}^*, \epsilon_{z0}, \epsilon_{z0}^*, \chi_x, \chi_y, \chi_{xy}, \chi_x^*, \chi_y^*, \chi_{xy}^*, \chi_z, \phi_x, \phi_y, \phi_x^*, \phi_y^*, \chi_{xz}, \chi_{yz}, \chi_{xz}^*, \chi_{yz}^*)^t$$

\underline{d} = vector of displacement variables per node defined at the mid-plane of the laminate

\underline{p}_o = load vector corresponding to displacement variables \underline{d}

The two-dimensional laminate constitutive relation is obtained as,

$$\bar{\underline{d}} = \underline{D}\bar{\underline{\epsilon}} \tag{13}$$

For the sake of brevity, further details are omitted here and the reader should consult References [12–19].

The theories based on the higher-order displacement models [Equations (1–6)] lead to nonvanishing transverse shear stresses on the top or bottom free bounding planes of the plate. The approach used so far [8,9] to satisfy the zero transverse shear conditions, i.e., γ_{xz} and γ_{yz} equal to zero at $z = \pm h/2$, is to modify the displacement model by incorporating these conditions and thus eliminate θ_x^* and θ_y^* [valid only for models given by Equations (1), (3) and (4)]. The resulting modified displacement model contains only the physical displacement components and their derivatives. But this leads to C^1 continuity in the finite element formulation. A different approach, which retains the C^0 continuity, is adopted here to incorporate the zero shear conditions. The shear rigidity matrix given by Equation (13) as against the displacement model is modified here as follows.

The conditions $(\gamma_{xz} \text{ and } \gamma_{yz})_{\pm h/2}$ equal to zero are substituted in Equation (7) and relations between θ_x and θ_x^* from γ_{xz} and between θ_y and θ_y^* from γ_{yz} are obtained. These relations are substituted in the shear rigidity matrix \underline{D}_s , such that the symmetric nature of \underline{D}_s is retained. This procedure is used for models with five, six and seven degrees of freedom given by Equations (1), (2) and (3) and these are designated as HOST5B, HOST6B and HOST7B, respectively [12,18].

The foregoing theories are used in conjunction with isoparametric finite elements in x - y plane. Lagrangian quadrilateral elements with 9 and 16 nodes are used. Selective numerical integration is employed for evaluating stiffness properties. The details are available elsewhere [19].

The evaluation of the interlaminar stresses $(\tau_{xz}, \tau_{yz}, \sigma_z)$ from the stress-strain constitutive relations given in Equation (12) leads to discontinuity at the interface of two adjacent layers of a laminate and thus violates the equilibrium conditions. The three-dimensional analysis becomes very complex due to the thickness variation of constitutive laws and continuity requirements across the interface. For this reason, the following equilibrium equations of elasticity for each layer are used to derive expressions for the interlaminar stresses in the L^h lamina of a multi-layered laminate.

$$\frac{\partial \sigma_x}{\partial x} + \frac{\partial \tau_{xy}}{\partial y} + \frac{\partial \tau_{xz}}{\partial z} = 0 \tag{14}$$

$$\frac{\partial \tau_{xy}}{\partial x} + \frac{\partial \sigma_y}{\partial y} + \frac{\partial \tau_{yz}}{\partial z} = 0 \tag{15}$$

$$\frac{\partial \tau_{xz}}{\partial x} + \frac{\partial \tau_{yz}}{\partial y} + \frac{\partial \sigma_z}{\partial z} = 0 \tag{16}$$

After substituting the lamina stresses in Equations (14) and (15), an integration is carried out to obtain the interlaminar shear stresses as,

$$\tau_{xz}^L \Big|_{z=h_{L+1}} = - \sum_{i=1}^L \int_{h_i}^{h_{i+1}} \left(\frac{\partial \sigma_x}{\partial x} + \frac{\partial \tau_{xy}}{\partial y} \right) dz + C_1 \tag{17}$$

$$\tau_{yz}^L|_{z=h_{L+1}} = - \sum_{i=1}^L \int_{h_i}^{h_{i+1}} \left(\frac{\partial \sigma_y}{\partial y} + \frac{\partial \tau_{xy}}{\partial x} \right) dz + C_2 \tag{18}$$

A second order differential equation is obtained for interlaminar normal stress in terms of inplane stresses after eliminating the interlaminar shear stresses from Equation (16), i.e.,

$$\frac{\partial^2 \sigma_z}{\partial z^2} = \frac{\partial^2 \sigma_x}{\partial x^2} + \frac{\partial^2 \sigma_y}{\partial y^2} + 2 \frac{\partial^2 \tau_{xy}}{\partial x \partial y} \tag{19}$$

The following equation is obtained for interlaminar normal stress after integrating Equation (19) twice,

$$\sigma_z^L|_{z=h_{L+1}} = \sum_{i=1}^L \int_{h_i}^{h_{i+1}} \left\{ \int_z \frac{\partial^2 \sigma_x}{\partial x^2} + \frac{\partial^2 \sigma_y}{\partial y^2} + 2 \frac{\partial^2 \tau_{xy}}{\partial x \partial y} dz \right\} dz + zC_3 + C_4 \tag{20}$$

Thus, it is seen that interlaminar stresses can be obtained by using stress equilibrium equations. But in Equations (17) and (18) for interlaminar shear stresses, it is seen that the values obtained may not in general satisfy both boundary conditions at $z = \pm h/2$, as only one constant of integration is present.

This problem does not arise in the case of σ_z , as here two constants of integration obtained by integrating twice, can be determined by substituting two boundary conditions at $z = \pm h/2$. The Equation (20) is solved as a boundary value problem instead of an initial value problem as in the case of Equations (17) and (18).

3. NUMERICAL RESULTS AND DISCUSSIONS

Performance of the two elements is demonstrated by comparing results for various laminate geometries with those obtained using elasticity, other laminate theory and finite element formulations. All computations were performed on a CYBER 180/840 computer in single precision with 16 significant digits as word-length. Due to biaxial symmetry of the problems discussed, only one quadrant of the laminate is analysed except for angle-ply and unsymmetric sandwich laminates which are analysed as full. The selective integration scheme based on Gauss-Legendre product rules, viz. 4×4 and 3×3 rule for flexure and shear contributions respectively for sixteen noded element and 3×3 and 2×2 rule for nine noded element to compute the element stiffness matrix is employed.

The following sets of data were used in obtaining the numerical results.

Material 1 [21]

$$\begin{aligned} E_1/E_2 &= 10 & G_{12}/E_2 &= 0.60 & G_{23}/E_2 &= 0.50 & E_2 &= E_3 \\ G_{13} &= G_{12} & \nu_{12} &= \nu_{23} = \nu_{13} & &= 0.25 & & \end{aligned}$$

Material 2 [23]

$$E_1/E_2 = 25 \quad G_{12}/E_2 = 0.50 \quad G_{23}/E_2 = 0.20 \quad E_2 = E_3$$

$$G_{13} = G_{12} \quad \nu_{12} = \nu_{23} = \nu_{13} = 0.25$$

Material 3 [23]*STIFF LAYERS*

$$E_1/E_2 = 25 \quad G_{12}/E_2 = 0.50 \quad G_{23}/E_2 = 0.20 \quad E_2 = E_3 = 10^6 \text{ psi}$$

$$G_{13} = G_{12} \quad \nu_{12} = \nu_{23} = \nu_{13} = 0.25 \quad h_s = 0.1 \text{ h}$$

CORE LAYERS

$$E_1 = E_2 = 0.4 \times 10^5 \text{ psi} \quad E_3 = 0.50 \times 10^6 \text{ psi}$$

$$G_{12} = G_{13} = 0.6 \times 10^5 \text{ psi}$$

$$G_{23} = 0.16 \times 10^5 \text{ psi} \quad \nu = 0.25$$

Material 4 [29]

$$E_1/E_2 = 40 \quad G_{12}/E_2 = 0.50 \quad G_{23}/E_2 = 0.60 \quad E_2 = E_3$$

$$G_{13} = G_{12} \quad \nu_{12} = \nu_{23} = \nu_{13} = 0.25$$

Material V [31]*FACE SHEETS*

$$E_1 = 1.308 \times 10^7 \text{ N/cm}^2 \quad E_2 = 1.06 \times 10^6 \text{ N/cm}^2$$

$$G_{12} = G_{13} = 6 \times 10^5 \text{ N/cm}^2$$

$$G_{23} = 3.9 \times 10^5 \text{ N/cm}^2 \quad \nu_{12} = \nu_{13} = 0.28 \quad \nu_{23} = 0.35$$

CORE

$$G_{23} = 1.772 \times 10^4 \text{ N/cm}^2 \quad G_{13} = 5.206 \times 10^4 \text{ N/cm}^2$$

(other properties are zero)

The deflection and interlaminar stresses are presented here in non-dimensional form using the following multipliers.

$$m_1 = \frac{10E_2h^3}{qa^4} \quad m_2 = \frac{h^2}{qa^2} \quad m_3 = \frac{h}{qa}$$

The superscripts e and c used in various tables that follow represent values of stresses obtained from equilibrium and constitutive relations, respectively.

Example 1. A simply supported orthotropic composite laminate under uniformly distributed load is considered. Material 1 set is used and the results for displacement and stresses are given in Table 1. The results show that the inplane and interlaminar stresses obtained from 16 noded element are close to the closed form solution [21] when compared to the 9 noded element results. But, transverse displacement results show that 9 noded element gives displacement which is better than 16 noded element when compared with closed form solution. Figure 1 shows the variation of interlaminar normal stress through the plate thickness. Since the closed form solution results are not available for comparison, these have been compared with the Mindlin theory [32] which show good agreement.

Example 2. A simply supported three layered symmetric cross-ply (0/90/0) square plate under sinusoidal transverse load is considered. Material 2 set is used and the numerical results for a/h ratios of 4, 10 and 100 are given respectively in Tables 2–4. The results show that the interlaminar shear stress τ_{yz} obtained by 16 noded element is close to the elasticity solution [23] compared to 9 noded element, but in the case of τ_{xz} , the vice-versa is seen for $a/h = 4$. For comparatively thin plates ($q/h = 10$) 16 noded element gives better results compared to 9 noded element. The displacement and inplane stress values show that 9 noded element gives accurate results for all values of a/h ratio. The variation of interlaminar normal stress through the laminate thickness is shown in Figure 2. This shows that the values obtained by present formulations match well with the elasticity solution [23].

Example 3. A simply supported three layered square orthotropic sandwich plate under sinusoidal transverse load is considered and Material 3 set is used. The numerical results for displacement and stresses are given in Tables 5–7 for a/h ratio 4, 10 and 100, respectively. The results show that the interlaminar shear stress τ_{yz} obtained by 16 noded element is close to elasticity solution [23], compared to 9 noded element for $a/h = 4$. But in the case of inplane stresses and the τ_{xz} vice-versa is seen. As the a/h ratio increases ($a/h = 10$) the stresses obtained by 16 noded element are close to elasticity solution and for thin laminate ($a/h = 100$) both elements almost give the same results when compared with elasticity solution. Since the elasticity solution results are not available for σ_z , these results are compared with the Mindlin theory [32] which is shown in Figures 4 and 5 for $a/h = 4$ and 10 respectively. This shows large difference in values for thick laminate ($a/h \leq 4$) and both theories converge almost to the same value when the laminate becomes thin ($a/h \geq 10$).

Example 4. A two layered unsymmetric cross-ply (0/90) square laminate subjected to sinusoidal loading is considered next for comparison of displacement and stresses. Material 2 set is used and numerical results are presented in Tables 9 and 10 for a/h ratios of 4 and 10 respectively. The results show that the τ_{yz} ,

Table 1. Maximum deflection, inplane and transverse shear stresses for orthotropic laminate under uniformly distributed load ($a/h = 5$).

Source	$\sigma_x \times m_2$	$\sigma_y \times m_2$	$\tau_{xz}^{(0)} \times m_3$	$\tau_{xz}^{(c)} \times m_3$	$\tau_{yz}^{(0)} \times m_3$	$\tau_{yz}^{(c)} \times m_3$	$\tau_{xy} \times m_2$	$w_o \times m_1$
HOST5A (9N)	0.6980	0.09448	0.5146	0.6134	0.16086	0.2216	0.12496	2.20144
HOST5A (16N)	0.6784	0.08784	0.6016	0.6050	0.18398	0.2146	0.12364	2.19644
HOST5B (9N)	0.6128	0.09344	0.4834	0.6326	0.15986	0.2288	0.12352	2.21296
HOST5B (16N)	0.6984	0.08816	0.5766	0.6180	0.18746	0.2166	0.12140	2.20578
HOST6A (9N)	0.6932	0.10056	0.5228	0.6072	0.17154	0.2238	0.12136	2.17455
HOST6A (16N)	0.6732	0.09484	0.6080	0.5998	0.19544	0.2168	0.12004	2.16606
HOST6B (9N)	0.6316	0.12700	0.5292	0.6368	0.32220	0.2552	0.10268	2.37395
HOST6B (16N)	0.7200	0.09568	0.5670	0.6118	0.19804	0.2188	0.11444	2.17834
FOST (9N)	0.6356	0.09236	0.5296	0.4208	0.16220	0.1498	0.11424	2.20640
FOST (16N)	0.6212	0.08652	0.6184	0.4142	0.18458	0.1448	0.11336	2.20320
MIF [21]	0.696935	0.100200	0.658798	—	0.277550	—	0.15847	2.22192
Ambartsumyan theory [25]	0.687582	0.094282	0.678002	—	0.279080	—	0.14158	2.20344
Reissner theory [2]	0.623231	0.097528	0.674894	—	0.282000	—	0.10739	2.17245

Table 2. Maximum deflection, inplane and transverse shear stresses for symmetric cross-ply laminate under sinusoidal loading (0/90/0) (a/h = 4).

Source	$\sigma_x \times m_2$	$\sigma_y \times m_2$	$\tau_{xy} \times m_2$	$\tau_{xz}^{\theta\theta} \times m_3$	$\tau_{xz}^{CC} \times m_3$	$\tau_{yz}^{\theta\theta} \times m_3$	$\tau_{yz}^{CC} \times m_3$	$\tau_{yz}^{\theta\theta} \times m_3$	$\tau_{yz}^{CC} \times m_3$	$w_0 \times m_1$
H0ST5A (9N)	0.77875	0.513938	0.050230	0.25125	0.20133	0.172325	0.17525	0.172325	0.17525	1.928125
H0ST5A (16N)	0.76750	0.507813	0.050048	0.29250	0.20150	0.204650	0.17483	0.204650	0.17483	1.927438
H0ST5B (9N)	0.70688	0.503188	0.049538	0.25975	0.19085	0.170100	0.18150	0.170100	0.18150	1.917813
H0ST5B (16N)	0.68813	0.506375	0.046144	0.30150	0.19080	0.202875	0.17900	0.202875	0.17900	1.918172
H0ST6A (9N)	0.77625	0.499813	0.048948	0.24915	0.43875	0.173325	0.17798	0.173325	0.17798	1.896969
H0ST6A (16N)	0.76500	0.493938	0.048781	0.28900	0.19945	0.204625	0.17575	0.204625	0.17575	1.896313
H0ST6B (9N)	0.68750	0.488063	0.045806	0.29850	0.18903	0.202850	0.18603	0.202850	0.18603	1.886219
H0ST6B (16N)	0.70625	0.486563	0.048531	0.25775	0.42025	0.170575	0.18398	0.170575	0.18398	1.886547
F0ST (9N)	0.56313	0.071438	0.043444	0.33900	0.13245	0.166875	0.13145	0.166875	0.13145	2.111563
F0ST (16N)	0.43750	0.477250	0.037106	0.35100	0.11678	0.191625	0.12615	0.191625	0.12615	1.776719
Exact [23]	0.801 -0.755	0.534 -0.556	-0.0511 0.0505	0.2560	—	0.2172	—	0.2172	—	2.006000
CFS [22]	0.831 -0.831	0.549 -0.549	-0.0526 0.0526	0.2330	—	0.2140	—	0.2140	—	2.014000
CLT [27,28]	-0.831 0.539	-0.549 0.180	-0.0526 0.0213	0.3950	—	0.0823	—	0.0823	—	—

Table 3. Maximum deflection, inplane and transverse shear stresses for symmetric cross-ply laminate under sinusoidal loading ($0/90/0$) ($a/h = 10$).

Source	$\sigma_x \times m_2$	$\sigma_y \times m_2$	$\tau_{xy} \times m_2$	$\tau_{xz}^{(0)} \times m_3$	$\tau_{xz}^{(c)} \times m_3$	$\tau_{yz}^{(0)} \times m_3$	$\tau_{yz}^{(c)} \times m_3$	$w_0 \times m_1$
HOST5A (9N)	0.5930	0.2742	0.02819	0.3249	0.2547	0.09701	0.09926	0.718250
HOST5A (16N)	0.5847	0.2711	0.02814	0.3838	0.2512	0.11460	0.09883	0.718034
HOST5B (9N)	0.5605	0.2693	0.02736	0.3289	0.2214	0.09566	0.10200	0.708230
HOST5B (16N)	0.5534	0.2669	0.02737	0.3895	0.2216	0.11300	0.10140	0.708066
HOST6A (9N)	0.5919	0.2735	0.02803	0.3244	0.5152	0.09767	0.10010	0.715600
HOST6A (16N)	0.5835	0.2704	0.02798	0.3830	0.2544	0.11520	0.09866	0.715600
HOST6B (9N)	0.5593	0.2685	0.02720	0.3283	0.4911	0.09606	0.10310	0.705766
HOST6B (16N)	0.5523	0.2663	0.02722	0.3888	0.2184	0.11340	0.10250	0.705627
FOST (9N)	0.5213	0.2562	0.02522	0.3370	0.1324	0.09142	0.07418	0.669860
FOST (16N)	0.5136	0.2534	0.02528	0.3986	0.1324	0.10820	0.07382	0.669690
Exact [23]	0.590	0.285	-0.0289	0.3570	—	0.12280	—	0.753000
	-0.590	-0.288	0.0289					
CFS [22]	0.594	0.288	-0.0291	0.3530	—	0.12200	—	0.755000
	-0.594	-0.288	0.0291					
MIF [29]	0.594	0.288	0.0291	0.3570	—	0.12300	—	0.754000

Table 4. Maximum deflection, inplane and transverse shear stresses for symmetric cross-ply laminate under sinusoidal loading ($0/90/0$) ($a/h = 100$).

Source	$\sigma_x \times m_2$	$\sigma_y \times m_2$	$\tau_{xy} \times m_2$	$\tau_{xz}^{(0)} \times m_3$	$\tau_{xz}^{(c)} \times m_3$	$\tau_{yz}^{(0)} \times m_3$	$\tau_{yz}^{(c)} \times m_3$	$w_0 \times m_1$
HOST5A (9N)	0.5446	0.1823	0.02155	0.3507	0.2710	0.06939	0.07108	0.434620
HOST5A (16N)	0.5384	0.1803	0.02132	0.4146	0.2681	0.08052	0.07126	0.434573
HOST5B (9N)	0.5443	0.1823	0.02154	0.3508	0.2307	0.06937	0.07416	0.434480
HOST5B (16N)	0.5380	0.1802	0.02131	0.4146	0.2288	0.08080	0.07435	0.434438
HOST6A (9N)	0.5446	0.1824	0.02155	0.3507	0.5859	0.06941	0.07108	0.434599
HOST6A (16N)	0.5384	0.1803	0.02132	0.4146	0.2721	0.08055	0.07052	0.434556
HOST6B (9N)	0.5443	0.1823	0.02154	0.3507	0.5126	0.06939	0.07417	0.434465
HOST6B (16N)	0.5380	0.1802	0.02131	0.4147	0.2317	0.08052	0.07345	0.434422
FOST (9N)	0.5439	0.1821	0.02152	0.3509	0.1367	0.06933	0.05672	0.434050
FOST (16N)	0.5376	0.1801	0.02129	0.4148	0.1373	0.08043	0.05687	0.434010
Exact [23]	0.539 -0.539	0.181 -0.181	-0.0213 0.0213	0.3950	—	0.08280	—	0.435000
CFS [22]	0.539 -0.539	0.181 -0.181	-0.0213 0.0213	0.3950	—	0.08280	—	0.435000
MIF [29]	0.539	0.181	0.0213	0.3850	—	0.08300	—	0.434000

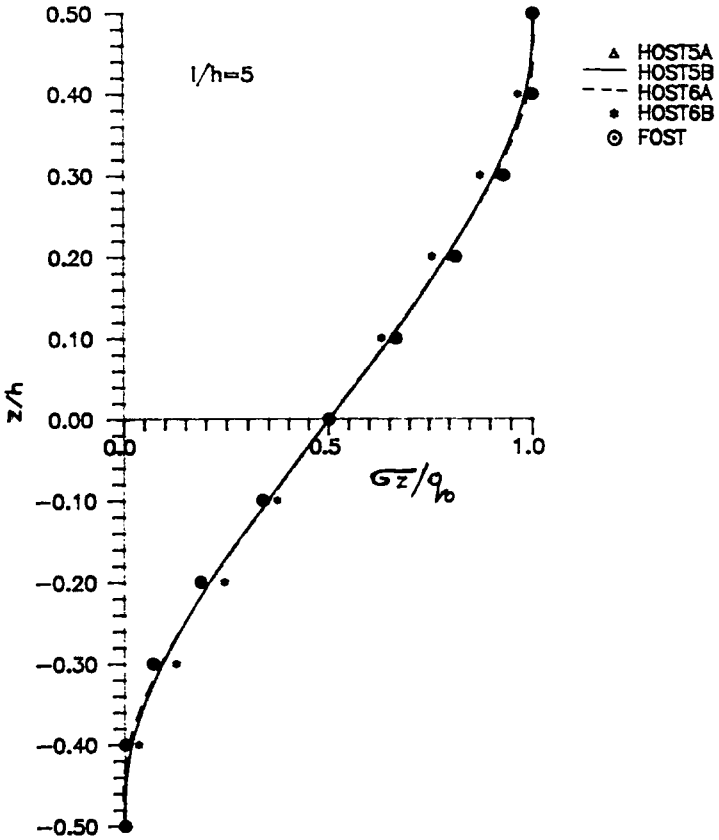


Figure 2. Variation of transverse normal stress through the thickness (orthotropic laminate) ($l/h = 5$).

Table 5. Maximum deflection, inplane and transverse shear stresses for symmetric sandwich laminate under sinusoidal loading ($a/h = 4$).

Source	$\sigma_x \times m_2$	$\sigma_y \times m_2$	$\tau_{xy} \times m_2$	$\tau_{xz}^{(0)} \times m_3$	$\tau_{xz}^{(c)} \times m_3$	$\tau_{yz}^{(0)} \times m_3$	$\tau_{yz}^{(c)} \times m_3$	$w_0 \times m_1$
HOST5A (9N)	1.52250	0.241375	0.141938	0.220075	0.27500	0.088975	0.113675	7.159688
HOST5A (16N)	1.50188	0.238875	0.141000	0.253750	0.26325	0.105550	0.113400	7.156172
HOST5B (9N)	1.24688	0.233813	0.134250	0.224525	0.23818	0.086525	0.113200	6.947344
HOST5B (16N)	1.24563	0.229938	0.132750	0.260000	0.23828	0.102900	0.112800	6.950109
HOST6A (9N)	1.53313	0.267125	0.138875	0.221875	0.27200	0.090200	0.113925	7.060156
HOST6A (16N)	1.51250	0.264313	0.138000	0.255000	0.22500	0.104775	0.113650	7.057516
HOST6B (9N)	1.31063	0.261500	0.099250	0.236925	0.23690	0.092875	0.119750	6.840688
HOST6B (16N)	1.27375	0.257375	0.130500	0.256500	0.23680	0.104150	0.137525	6.852109
FOST (9N)	0.90563	0.157813	0.091190	0.250500	0.09953	0.066025	0.043575	4.767969
FOST (16N)	0.89250	0.156188	0.091000	0.292750	0.09953	0.077975	0.043375	4.766563
Exact [23]	1.556	0.2595	-0.1437	0.23900	—	0.10720	—	7.596000
	-1.512	-0.2533	0.1481					
CFS [22]	1.556	0.2519	0.1480	0.23800	—	0.10590	—	7.654000
	-1.556	-0.2519	-0.1480					

Table 6. Maximum deflection, inplane and transverse shear stresses for symmetric sandwich laminate under sinusoidal loading ($a/h = 10$).

Source	$\sigma_x \times m_2$	$\sigma_y \times m_2$	$\tau_{xy} \times m_2$	$\tau_{xz}^{(b)} \times m_3$	$\tau_{xz}^{(c)} \times m_3$	$\tau_{yz}^{(b)} \times m_3$	$\tau_{yz}^{(c)} \times m_3$	$w_0 \times m_1$
HOST5A (9N)	1.1660	0.10520	0.06915	0.2685	0.3400	0.044620	0.05642	2.08650
HOST5A (16N)	1.1490	0.10410	0.06897	0.3162	0.3403	0.052320	0.05608	2.08571
HOST5B (9N)	1.1100	0.10520	0.06660	0.2700	0.2841	0.004366	0.05593	2.02250
HOST5B (16N)	1.0910	0.10070	0.06645	0.3182	0.2842	0.051111	0.05557	2.02242
HOST6A (9N)	1.1680	0.11110	0.06888	0.2676	0.3393	0.044070	0.05422	2.08162
HOST6A (16N)	1.1520	0.10990	0.06870	0.3152	0.3395	0.051930	0.05610	2.08081
HOST6B (9N)	1.1140	0.10770	0.06637	0.2691	0.2724	0.043230	0.05631	2.01793
HOST6B (16N)	1.0950	0.10680	0.06623	0.3171	0.2839	0.050590	0.05597	2.01788
FOST (9N)	1.0620	0.08058	0.05533	0.2780	0.1112	0.036360	0.02383	1.56130
FOST (16N)	1.0460	0.07973	0.05538	0.3285	0.1113	0.042380	0.02366	1.56090
Exact [23]	1.153	0.1104	-0.0707	0.30000	—	0.052700	—	2.20000
	-1.152	-0.1099	0.0717					
CFS [22]	1.154	0.1092	-0.0714	0.30000	—	0.052400	—	2.20400
	-1.154	-0.1092	0.0714					

Table 7. Maximum deflection, inplane and transverse shear stresses for symmetric sandwich laminate under sinusoidal loading ($a/h = 100$).

Source	$\sigma_x \times m_2$	$\sigma_y \times m_2$	$\tau_{xy} \times m_2$	$\tau_{xz}^{(H)} \times m_3$	$\tau_{xz}^{(C)} \times m_3$	$\tau_{yz}^{(H)} \times m_3$	$\tau_{yz}^{(C)} \times m_3$	$w_o \times m_1$
HOST5A (9N)	1.1090	0.05539	0.04399	0.2880	0.3627	0.02704	0.33220	0.891480
HOST5A (16N)	1.0960	0.05477	0.04356	0.3406	0.3641	0.03056	0.33260	0.891381
HOST5B (9N)	1.1080	0.05535	0.04396	0.2880	0.3001	0.02703	0.33620	0.890720
HOST5B (16N)	1.0950	0.05473	0.04353	0.3407	0.3013	0.03054	0.33660	0.890625
HOST6A (9N)	1.1100	0.5645	0.04400	0.2878	0.3627	0.02676	0.32990	0.891730
HOST6A (16N)	1.0970	0.05581	0.04357	0.3405	0.3641	0.03021	0.33040	0.891629
HOST6B (9N)	1.1100	0.05641	0.04397	0.2879	0.3002	0.02675	0.33540	0.890976
HOST6B (16N)	1.0970	0.05577	0.04354	0.3405	0.3014	0.03019	0.33580	0.890875
FOST (9N)	1.1070	0.05510	0.04385	0.2882	0.1144	0.02697	0.17220	0.885560
FOST (16N)	1.0950	0.05448	0.04339	0.3408	0.1149	0.03042	0.03413	0.885560
Exact [23]	1.098	0.0550	-0.0437	0.3240	—	0.02970	—	0.892000
	-1.098	-0.0550	0.0437					
CFS [22]	1.098	0.0550	0.0437	0.3240	—	0.02970	—	0.892000
	-1.098	-0.0550	-0.0437					

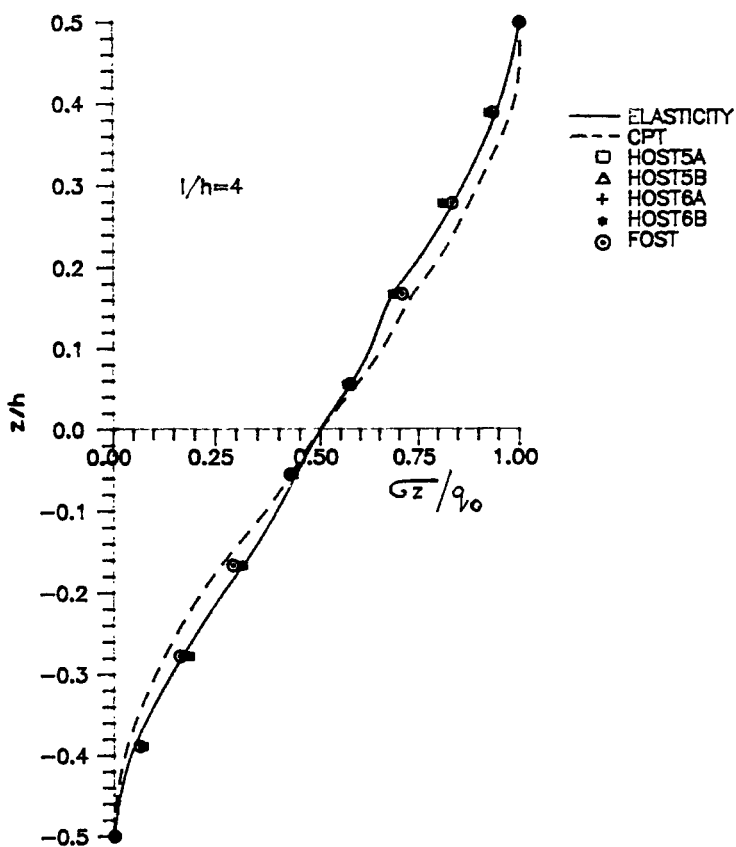


Figure 3. Variation of transverse normal stress through the thickness (0/90/0) ($l/h = 4$).

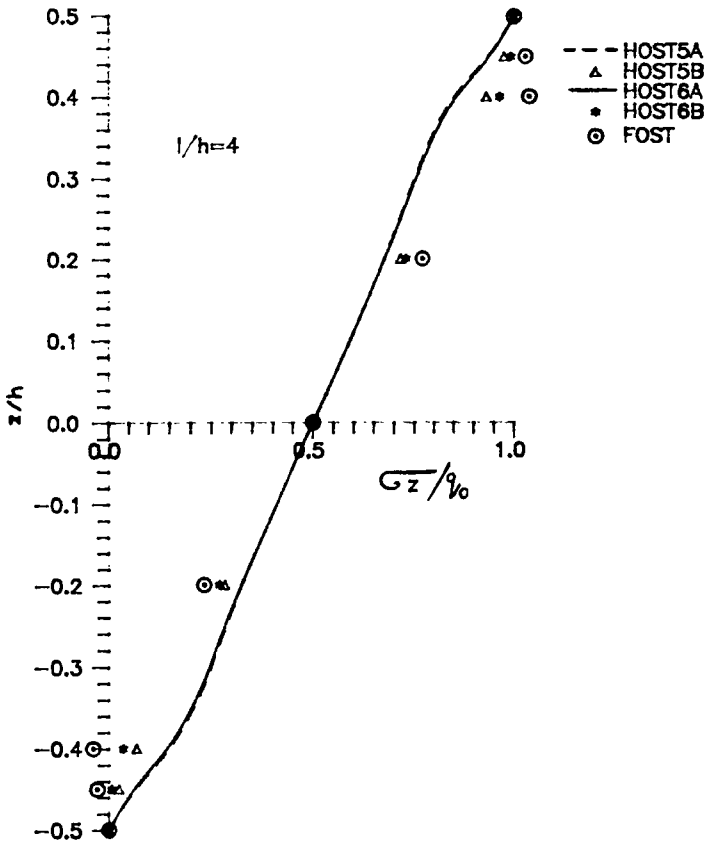


Figure 4. Variation of transverse normal stress through the thickness (sandwich laminate) ($l/h = 4$).

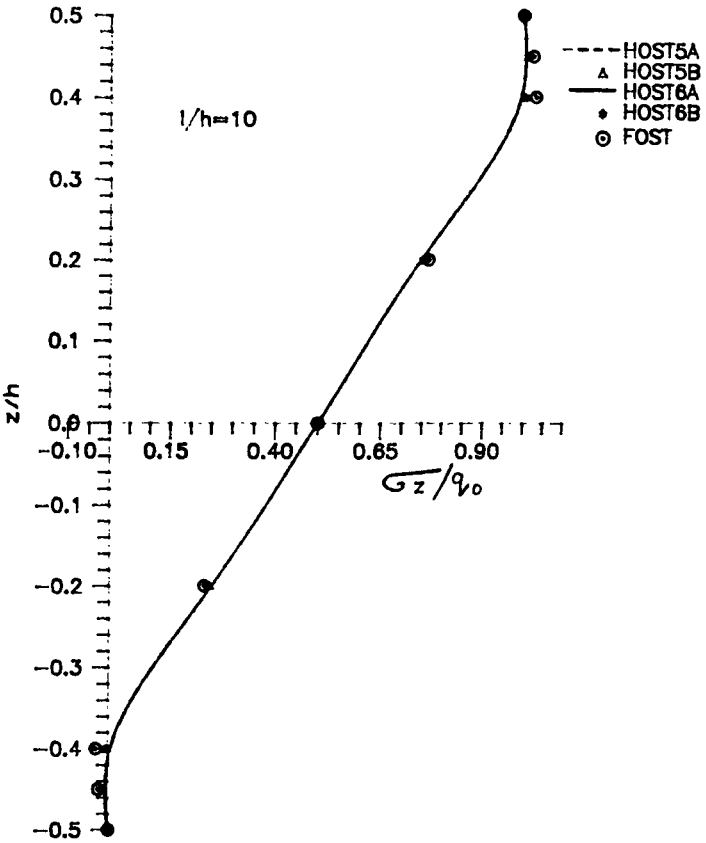


Figure 5. Variation of transverse normal stress through the thickness (sandwich laminate) ($l/h = 10$).

Table 8. Maximum deflection, inplane and transverse shear stresses for unsymmetric cross-ply laminate under sinusoidal loading ($0/90$) ($a/h = 4$).

Source	$\sigma_x \times m_2$	$\sigma_y \times m_2$	$\tau_{xy} \times m_2$	$\tau_{yz} \times m_2$	$\tau_{xz}^{90} \times m_3$	$\tau_{xz}^{CC} \times m_3$	$\tau_{yz}^{90} \times m_3$	$\tau_{yz}^{CC} \times m_3$	$w_o \times m_1$
HOST7A (9N)	0.08819 -0.84250	0.84250 -0.08819	-0.055725 0.055725	-0.055725 0.055725	0.29600	0.25275	0.29050	0.27500	2.032656
HOST7A (16N)	0.08713 -0.87000	0.87000 -0.08713	-0.055888 0.055888	-0.055888 0.055888	0.34900	0.27500	0.34900	0.27500	2.032188
HOST7B (9N)	0.09263 -1.01813	1.01813 -0.09263	-0.059950 0.059950	-0.059950 0.059950	0.30050	0.21228	0.29575	0.27850	1.956250
HOST7B (16N)	0.09100 -0.99688	0.99688 -0.09100	-0.058681 0.058681	-0.058681 0.058681	0.35275	0.21165	0.35450	0.21165	1.954688
HOST9 (9N)	0.09694 -0.80563	0.80563 -0.09694	-0.059663 0.059663	-0.059663 0.059663	0.29025	0.27000	0.28450	0.28375	2.055469
HOST9 (16N)	0.09588 -0.79313	0.79313 -0.09588	-0.059538 0.059538	-0.059538 0.059538	0.33775	0.26975	0.34150	0.28350	2.055000
HOST11 (9N)	0.11100 -0.77813	0.82188 -0.09975	-0.057669 0.057894	-0.057669 0.057894	0.28725	0.27150	0.28375	0.27675	2.032813

(continued)

Table 8. (continued).

Source	$\sigma_x \times m_2$	$\sigma_y \times m_2$	$\tau_{xy} \times m_2$	$\tau_{xz}^{(0)} \times m_3$	$\tau_{xz}^{(c)} \times m_3$	$\tau_{yz}^{(0)} \times m_3$	$\tau_{yz}^{(c)} \times m_3$	$w_0 \times m_1$
HOST11 (16N)	0.11063 -0.76250	0.81250 -0.09738	-0.057681 0.057725	0.33750	0.27150	0.35600	0.26800	2.031250
HOST12 (9N)	0.11169 -0.77813	0.82188 -0.09944	-0.057650 0.057650	0.28775	0.27175	0.28400	0.28075	2.032813
HOST12 (16N)	0.11119 -0.76188	0.81313 -0.09700	-0.057719 0.057663	0.33700	0.27150	0.34600	0.26825	2.031250
FOST (9N)	0.08525 -0.72438	0.72438 -0.08525	-0.052750 0.052750	0.29825	0.22100	0.29225	0.22100	2.149844
FOST (16N)	0.08425 -0.71500	0.71500 -0.08425	-0.052681 0.052681	0.34800	0.22085	0.35152	0.22085	2.149375
Exact [23]	0.10980 -0.78070	0.84170 -0.09550	-0.058800 0.059100	0.31270	—	0.31880	—	—
CFS [22]	0.09840 -0.83360	0.83360 -0.09840	-0.061200 0.061200	0.325400	—	0.32580	—	—

Table 9. Maximum deflection, inplane and transverse shear stresses for unsymmetric cross-ply laminate under sinusoidal loading ($a/h = 10$).

Source	$\sigma_x \times m_2$	$\sigma_y \times m_2$	$\tau_{xy} \times m_2$	$\tau_{xz}^{\theta} \times m_3$	$\tau_{xz}^{cc} \times m_3$	$\tau_{yz}^{\theta} \times m_3$	$\tau_{yz}^{cc} \times m_3$	$w_0 \times m_1$
HOST7A (9N)	0.08576 -0.74520	0.74520 -0.08576	0.05330 -0.05330	0.2980	0.2564	0.2922	0.2811	1.2203
HOST7A (16N)	0.08475 -0.73560	0.73560 -0.08475	0.05311 -0.05311	0.3476	0.2565	0.3513	0.2811	1.2201
HOST7B (9N)	0.08617 -0.76770	0.76440 -0.08617	0.05421 -0.05421	0.2975	0.2780	0.2917	0.3178	1.2128
HOST7B (16N)	0.08531 -0.75880	0.75880 -0.08531	0.05362 -0.05362	0.3476	0.2782	0.3513	0.3179	1.2124
HOST9 (9N)	0.08711 -0.73900	0.73900 -0.08711	0.05399 -0.05399	0.2972	0.2728	0.2914	0.2880	1.2237
HOST9 (16N)	0.08618 -0.72870	0.72870 -0.08618	0.05368 -0.05368	0.3463	0.2729	0.3501	0.2881	1.2236

(continued)

Table 9. (continued).

Source	$\sigma_x \times m_2$	$\sigma_y \times m_2$	$\tau_{xy} \times m_2$	$\tau_{xz}^{(0)} \times m_3$	$\tau_{xz}^{cc} \times m_3$	$\tau_{yz}^{(0)} \times m_3$	$\tau_{yz}^{cc} \times m_3$	$w_0 \times m_1$
HOST11 (9N)	0.08949 -0.73550	0.73670 -0.08749	0.05362 -0.05378	0.2974	0.2735	0.2898	0.2816	1.2200
HOST11 (16N)	0.08866 -0.72500	0.72690 -0.08640	0.05332 -0.05350	0.3467	0.2736	0.3509	0.2869	1.2200
HOST12 (9N)	0.08951 -0.73550	0.73670 -0.08747	0.05362 -0.05378	0.2974	0.2735	0.2898	0.2868	1.2200
HOST12 (16N)	0.08867 -0.72500	0.72690 -0.08639	0.05332 -0.05350	0.3467	0.2736	0.3509	0.2869	1.2200
FOST (9N)	0.08522 -0.72400	0.72400 -0.08522	0.05278 -0.05278	0.2983	0.2209	0.2924	0.2209	1.2378
FOST (16N)	0.08424 -0.71520	0.71520 -0.08424	0.05256 -0.05256	0.3480	0.2208	0.3517	0.2208	1.2377
Exact [23]	0.08900 -0.73000	— —	-0.05360 0.05380	0.3310	—	—	—	—
CFS [22]	0.08700 -0.73400	— —	-0.05400 0.05400	0.3320	—	—	—	—

Table 10. Maximum deflection, inplane and transverse shear stresses for unsymmetric angle-ply laminate under sinusoidal loading (15/-15) (a/h = 10).

Source	$\sigma_x \times m_2$	$\sigma_y \times m_2$	$\tau_{xy} \times m_2$	$\tau_{xz}^{\theta\theta} \times m_3$	$\tau_{xz}^{cc} \times m_3$	$\tau_{yz}^{\theta\theta} \times m_3$	$\tau_{yz}^{cc} \times m_3$	$w_o \times m_1$
HOST7A (9N)	0.6263	0.07640	-0.1466	0.3055	0.2998	0.74830	0.06627	0.62360
	-0.6216	-0.07644	0.1448					
HOST7A (16N)	0.6190	0.07554	-0.1449	0.3609	0.3001	0.08017	0.06083	0.62359
	-0.6135	-0.07563	0.1428					
HOST7B (9N)	0.6448	0.07748	-0.1518	0.3044	0.3186	0.07453	0.07097	0.61948
	-0.6394	-0.07757	0.1497					
HOST7B (16N)	0.6555	0.07853	-0.1545	0.3597	0.3185	0.07995	0.07062	0.61951
	-0.6491	-0.07863	0.1521					
HOST9 (9N)	0.6250	0.07692	-0.1448	0.3054	0.3036	0.07347	0.06983	0.63779
	-0.6211	-0.07703	0.1431					
HOST9 (16N)	0.6178	0.07603	-0.1431	0.3623	0.3040	0.07833	0.06958	0.63774
	-0.6133	-0.07621	0.1412					

(continued)

Table 10. (continued).

Source	$\sigma_x \times m_2$	$\sigma_y \times m_2$	$\tau_{xy} \times m_2$	$\tau_{xz}^{\theta} \times m_3$	$\tau_{xz}^{cc} \times m_3$	$\tau_{yz}^{\theta} \times m_3$	$\tau_{yz}^{cc} \times m_3$	$W_o \times m_1$
HOST11 (9N)	0.6250 -0.6175	0.07910 -0.07712	-0.1442 0.1423	0.3039	0.3025	0.07386	0.06633	0.63430
HOST11 (16N)	0.6177 -0.6101	0.07802 -0.07643	-0.1426 0.1405	0.3593	0.3018	0.07836	0.06941	0.63430
HOST12 (9N)	0.6249 -0.6175	0.07909 -0.07713	-0.1423 0.1442	0.3039	0.3026	0.07386	0.06633	0.64330
HOST12 (16N)	0.6177 -0.6100	0.07811 -0.07642	-0.1426 0.1404	0.3593	0.3019	0.07832	0.06502	0.63430
FOST (9N)	0.5867 -0.5823	0.07372 -0.07380	-0.1360 0.1343	0.3068	0.2524	0.07538	0.05652	0.63647
FOST (16N)	0.5803 -0.5750	0.07292 -0.07303	-0.1345 0.1325	0.3625	0.2526	0.08083	0.05629	0.63646
CFS [26]	0.6250 0.6250	-0.07700 -0.07700	-0.1460 0.1460	0.27090	—	0.07300	—	0.64760

values obtained with 16 noded element is close to the elasticity solution [23] compared to 9 noded element and for other stresses vice-versa is seen for $a/h = 4$. But for $a/h = 10$ the 16 noded element gives better estimates for all the stresses. The variation of interlaminar normal stress through the laminate thickness for $a/h = 4$ is shown in Figure 5. The results show that the present theories follow a different path compared to the elasticity solution [23] but converge to the same value at the bottom and top where the load is applied.

Example 5. A two layered simply supported unsymmetric angle-ply (15/ - 15) square plate subjected to sinusoidal loading is considered. Material 4 set is used and the results are given in Table 10 for $a/h = 10$. The results show that the displacement, inplane and interlaminar stresses obtained by 9 noded element match well with the closed form solution [29] compared to the 16 noded element. Since the closed form solution results were not available for interlaminar normal stress,

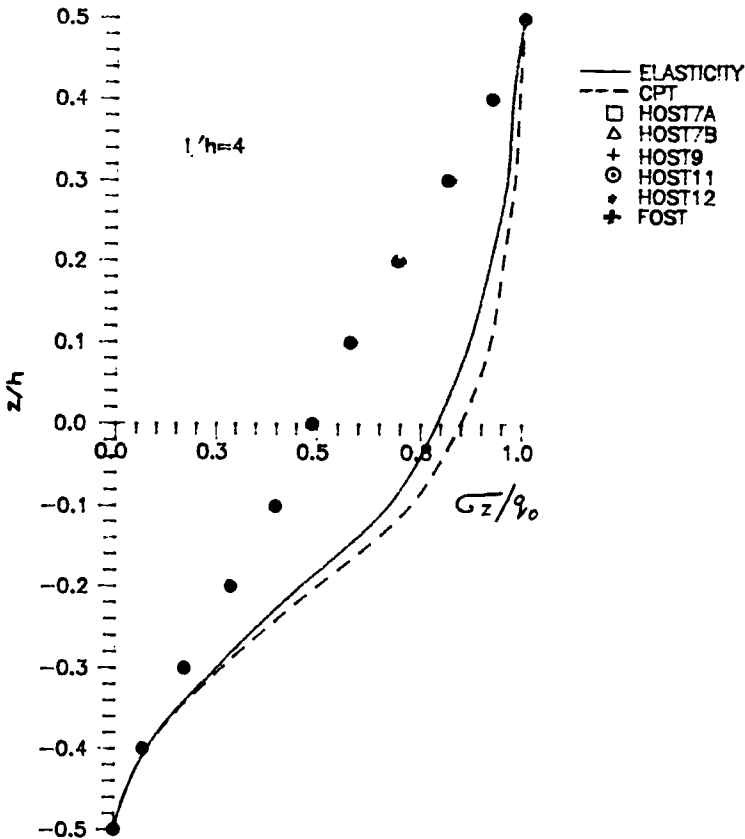


Figure 6. Variation of transverse normal stress through the thickness (σ_z/σ_0) ($l/h = 4$).

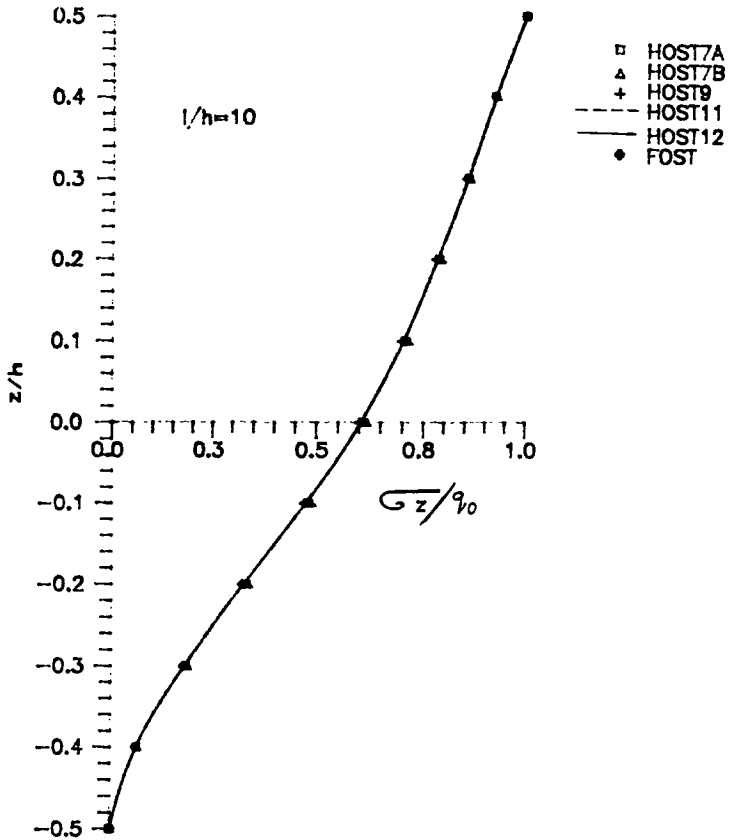


Figure 7. Variation of transverse normal stress through the thickness (15/ - 15) ($l/h = 10$).

they have been compared with Mindlin theory [32] (Figure 7) which show good agreement.

Example 6. A clamped unsymmetrical 8 layered sandwich plate (0/90/30/core/30/-45/45/0) under uniformly distributed load is considered and Material 5 set is used. The results for displacement, inplane and interlaminar stresses for $a/h = 10$ and 50 are presented in Tables 10 and 11 respectively and the variation of interlaminar normal stress through the plate thickness is shown in Figures 8 and 9 for $a/h = 10$ and 50 respectively. The results show large difference in displacement, inplane and interlaminar stresses for thick laminate ($a/h \leq 10$) compared to the Mindlin theory. This is because of the simplifying assumptions made in the Mindlin theory. But for the thin laminates ($a/h \geq 50$) both the theories give almost the same results.

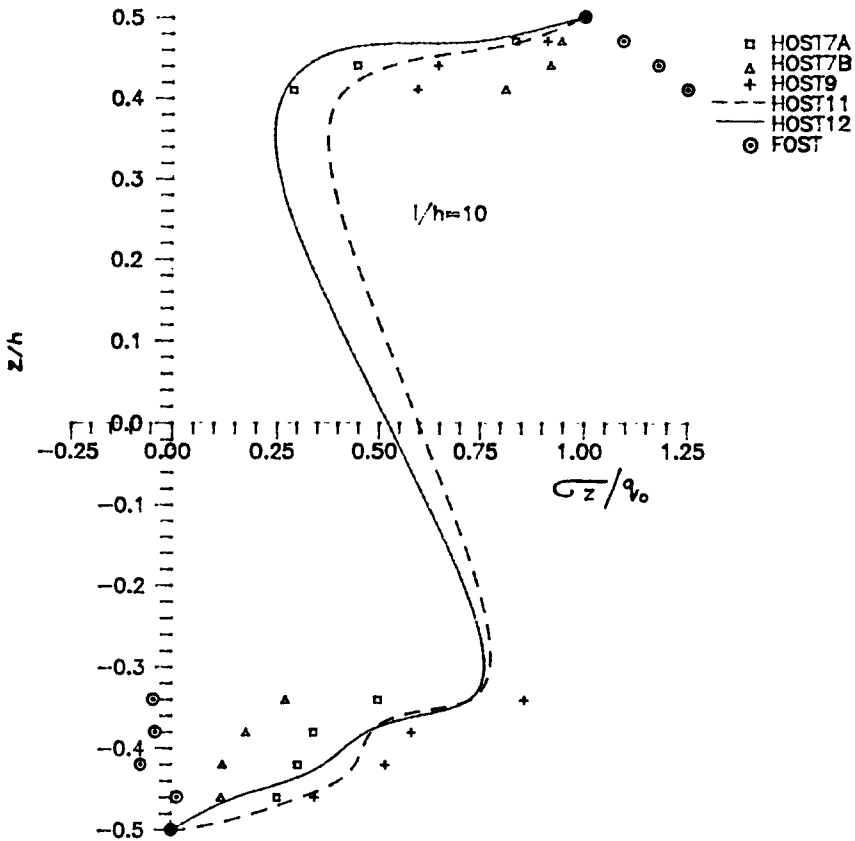


Figure 8. Variation of transverse normal stress through the thickness (sandwich laminate) ($l/h = 10$).

Table 11. Maximum deflection, inplane and transverse shear stresses for unsymmetric sandwich laminate under uniformly distributed load ($a/h = 10$) (0/90/30/core/30/-45/45/0).

Source	$\sigma_x \times m_2$	$\sigma_y \times m_2$	$\tau_{xy} \times m_2$	$\tau_{xz}^{(0)} \times m_3$	$\tau_{xz}^{(c)} \times m_3$	$\tau_{yz}^{(0)} \times m_3$	$\tau_{yz}^{(c)} \times m_3$	$W_o \times m_1$
HOST7A (9N)	0.8998	0.4299	0.1788	0.3322	0.3355	0.1753	0.15690	2.006156
HOST7A (16N)	0.7347	0.3723	0.2131	0.3965	1.0500	0.2113	0.14240	1.884892
HOST7B (9N)	0.7917	0.4997	0.1797	0.3227	0.2965	0.2249	0.10720	1.719426
HOST7B (16N)	0.6504	0.4212	0.2006	0.3449	0.2903	0.2477	0.10590	1.921780
HOST9 (9N)	0.9014	0.4143	0.1796	0.3929	0.9575	0.1934	0.85460	2.053750
HOST9 (16N)	0.7406	0.3592	0.1882	0.3699	0.3217	0.2091	0.14680	1.925808
HOST11 (9N)	0.9258	0.4302	0.1788	0.3884	0.9372	0.1947	0.84360	2.048980
HOST11 (16N)	0.7566	0.3771	0.7894	0.4051	0.8866	0.2058	0.14650	1.923900
HOST12 (9N)	0.9367	0.4423	0.1797	0.3754	0.8503	0.1791	0.16340	2.057460
HOST12 (16N)	0.7402	0.3886	0.2004	0.3731	0.3279	0.2048	0.14790	1.930260
FOST (9N)	0.6803	0.5352	0.1885	0.3297	0.1088	0.2489	0.03691	1.112364
FOST (16N)	0.6342	0.4828	0.1808	0.3415	0.1078	0.2677	0.03641	1.201934

Table 12. Maximum deflection, inplane and transverse shear stresses for unsymmetric sandwich laminate under uniformly distributed load ($a/h = 50$) (0/90/30/core/30/-45/45/0).

Source	$\sigma_x \times m_2$	$\sigma_y \times m_2$	$\tau_{xy} \times m_2$	$\tau_{xz}^{(0)} \times m_3$	$\tau_{yz}^{(0)} \times m_3$	$\tau_{xz}^{(c)} \times m_3$	$\tau_{yz}^{(c)} \times m_3$	$w_0 \times m_1$
H0ST7A (9N)	0.7280	0.4816	0.19760	0.3524	0.3900	0.2432	0.23460	0.560757
H0ST7A (16N)	0.6744	0.4160	0.18224	0.3888	0.3568	0.2692	0.20740	0.598569
H0ST7B (9N)	0.7056	0.4892	0.20040	0.3504	0.3240	0.2500	0.13134	0.544068
H0ST7B (16N)	0.6672	0.4320	0.18200	0.3836	0.3304	0.2772	0.13962	0.599502
H0ST9 (9N)	0.7284	0.4792	0.19784	0.3524	0.3984	0.2422	0.24640	0.563615
H0ST9 (16N)	0.6760	0.4144	0.18256	0.3890	0.3646	0.2680	0.21740	0.600588
H0ST11 (9N)	0.7256	0.4776	0.19704	0.3596	0.3986	0.2534	0.24620	0.560698
H0ST11 (16N)	0.6788	0.4196	0.18296	0.3956	0.3642	0.2780	0.21760	0.597501
H0ST12 (9N)	0.7252	0.4772	0.19704	0.3596	0.3990	0.2534	0.24640	0.560698
H0ST12 (16N)	0.6768	0.4036	0.18300	0.3956	0.3646	0.2780	0.21780	0.597501
F0ST (9N)	0.7052	0.4984	0.19764	0.3498	0.1207	0.2530	0.04098	0.516262
F0ST (16N)	0.6640	0.4356	0.17464	0.3866	0.1240	0.2842	0.04198	0.567660

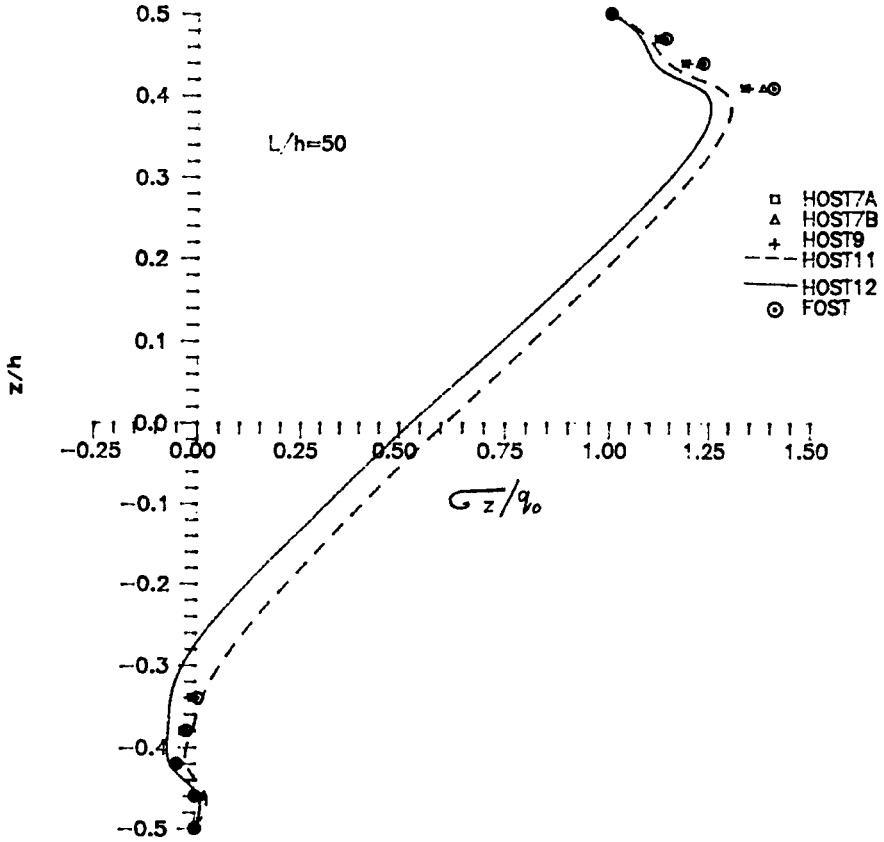


Figure 9. Variation of transverse normal stress through the thickness (sandwich laminate) ($l/h = 50$).

4. CONCLUSIONS

In summary, a number of simple but accurate and efficient C° finite element higher-order theories have been presented. These theories do not require the usual shear correction coefficient(s) which is/are generally associated with the first-order shear deformable theories of Mindlin and Reissner. Element tests have been performed in the linear range for comparison with closed form elasticity and other numerical solutions. Computed displacements and stresses are in excellent agreement with those obtained by elasticity for a variety of laminate geometries and loading. Convergence has been demonstrated by considering various a/h refinements. Interlaminar normal stress is presented and compared with elasticity solution which shows good agreement for the symmetric case. For the unsymmetric case it follows a different path, but converges to the same values

at top and bottom of the plate. This may be due to the use of third derivative of displacements which is reflected in the unsymmetric case. For the other problems also these results have been given which can be used for future reference. This is possible only by taking cubic variation of displacement as the third derivatives of displacements can be calculated. Thus 16 noded element has been used in these formulations and this can be used when all the stresses are to be evaluated. The results obtained by models when the zero shear conditions on top and bottom surfaces are not satisfied are better compared to the models when this condition is satisfied for thick laminates.

In the symmetric case, the results of HOST6 are most reliable and close to the closed form and elasticity solutions compared to other models, as this model considers the nonlinear variation of transverse displacements. Hence this model is most suited to tackle symmetric composite and sandwich plates.

In the unsymmetric case, the results of HOST9 are reliable and close to the closed form and elasticity solution compared to the other models for composites. Thus, this model is recommended for the evaluation of stresses in composite plates, but for sandwich plates and other highly anisotropic composite plates HOST12 may be used, as this model takes care of the three-dimensional effects and fairly realistic variation of displacements in thick laminates.

REFERENCES

1. Jones, R. M. 1975. *Mechanics of Composite Materials*. New York: McGraw-Hill.
2. Reissner, E. 1945. "The Effect of Transverse Shear Deformation on the Bending of Elastic Plates," *ASME J. Appl. Mech.*, 12:A69-A77.
3. Mindlin, R. D. 1951. "Influence of Rotatory Inertia and Shear Deformation on Flexural Motions of Isotropic Elastic Plates," *ASME J. Appl. Mech.*, 18:31-38.
4. Reissner, E. 1975. "On Transverse Bending of Plates Including the Effect of Transverse Shear Deformation," *Int. J. Solids Struct.*, 11:569-573.
5. Lo, K. H., R. M. Christensen and E. M. Wu. 1977. "A Higher Order Theory of Plate Deformation—Part 2: Laminated Plates," *ASME J. Appl. Mech.*, 44:669-676.
6. Kant, T. 1982 "Numerical Analysis of Thick Plates," *Comput. Meth. Appl. Mech. Engg.*, 31:1-18.
7. Kant, T., D. R. J. Owen and O. C. Zienkiewicz. 1982. "A Refined Higher Order C^0 Plate Bending Element," *Comput. Struct.*, 15:177-183.
8. Murthy, M. V. V. 1981. "An Improved Transverse Shear Deformation Theory for Laminated Anisotropic Plates," NASA Technical Paper-1903.
9. Reddy, J. N. 1984. "A Simple Higher Order Theory for Laminated Composite Plates," *ASME J. Appl. Mech.*, 51:745-752.
10. Phan, N. D. and J. N. Reddy. 1985. "Analysis of Laminated Composite Plates Using a Higher Order Shear Deformable Theory," *Int. J. Numer. Meth. Engg.*, 21:2201-2219.
11. Pucha, N. S. and J. N. Reddy. 1986. "A Refined Mixed Shear Flexible Finite Element for the Non-Linear Analysis of Laminated Plates," *Comput. Struct.*, 22:529-538.
12. Pandya, B. N. and T. Kant. 1987. "A Consistent Refined Theory for Flexure of a Symmetric Laminate," *Mech. Res. Commun.*, 14:107-113.
13. Pandya, B. N. and T. Kant. 1988. "Flexure Analysis of Laminated Composites Using Refined Higher Order C^0 Plate Bending Elements," *Comput. Meth. Appl. Mech. Engg.*, 66:173-198.
14. Pandya, B. N. and T. Kant. 1988. "A Refined Higher Order Generally Orthotropic C^0 Plate Bending Element," *Comput. Struct.*, 28:119-133.

15. Pandya, B. N. and T. Kant. 1988. "A Simple Finite Element Formulation of a Higher Order Theory for Unsymmetrically Laminated Composite Plates," *Compos. Struct.*, 9:215-246.
16. Pandya, B. N. and T. Kant. 1988. "Finite Element Stress Analysis of Laminated Composite Plates Using a Higher Order Displacement Model," *Compos. Sci. Technol.*, 32:137-155.
17. Kant, T. and B. N. Pandya. 1988. "Finite Element Stress Analysis of Unsymmetrically Laminated Composite Plates Based on a Refined Higher Order Theory," in *Composite Materials and Structures*, K. A. V. Pandalai and S. K. Malhotra, eds., New Delhi: Tata McGraw-Hill, pp. 373-380.
18. Pandya, B. N. and T. Kant. 1988. "Higher Order Shear Deformable Theories for Flexure of Sandwich Plates—Finite Element Evaluations," *Int. J. Solids Struct.*, 24(12):1267-1286.
19. Kant, T. and B. S. Manjunatha. 1988. "An Unsymmetric FRC Laminate C^0 Finite Element Model with Twelve Degrees of Freedom Per Node," *Int. J. Engg. Computat.*, 5(4):300-308.
20. Turvey, G. J. 1977. "Bending of Laterally Loaded, Simply Supported, Moderately Thick, Antisymmetrically Laminated Rectangular Plates," *Fiber Sci. Technol.*, 10:211-232.
21. Iyengar, K. T. S. and S. K. Pandya. 1983. "Analysis of Orthotropic Rectangular Thick Plates," *Fibre Sci. Technol.*, 18:19-36.
22. Ren, J. G. 1987. "A New Theory of Laminated Plate," *Compos. Sci. Technol.*, 26:225-239.
23. Pagano, N. J. 1970. "Exact Solution for Rectangular Bidirectional Composites and Sandwich Plates," *J. Compos. Mater.*, 4:20-34.
24. Pagano, N. J. 1969. "Exact Solution for Composite Laminates in Cylindrical Bending," *J. Compos. Mater.*, 3:398-411.
25. Ambartsumyan, S. A. 1970. *Theory of Anisotropic Plates*. Lancaster, PA: Technomic Publishing Co., Inc.
26. Ren, J. G. 1987. "Bending of Simply Supported, Antisymmetrically Laminated Rectangular Plate under Transverse Loading," *Compos. Sci. Technol.*, 28:231-243.
27. Reissner, E. and Y. Stavsky. 1961. "Bending and Stretching of Certain Types of Heterogeneous Aeolotropic Elastic Plates," *ASME J. Appl. Mech.*, 28:402-408.
28. Stavsky, Y. 1961. "Bending and Stretching of Laminated Aeolotropic Plates," *ASCE J. Engg. Mech.*, 87:31-56.
29. Iyengar, K. T. S. and S. K. Pandya. 1986. "Application of the Method of Initial Functions for the Analysis of Composite Laminated Plates," *Ing. Arch.*, 56:407-416.
30. Reddy, J. N. and W. C. Chao. 1981. "A Comparison of Closed Form and Finite Element Solutions of Thick Laminated Anisotropic Rectangular Plates," *Nucl. Engg. Des.*, 64:153-167.
31. Chirns, D. S. and P. A. Lagace. 1987. "Thick Composite Plates Subjected to Lateral Loading," *ASME J. Appl. Mech.*, 54:611-616.
32. Kant, T. and Mallikarjuna. 1989. "Transient Dynamics of Composite Sandwich Plates Using 4-, 8-, 9-Noded Isoparametric Quadrilateral Elements," *Finite Elements in Analysis and Design*, 6:307-318.